An unusual fold for potassium channel blockers: NMR structure of three toxins from the scorpion *Opisthacanthus madagascariensis*

Benjamin CHAGOT*, Cyril PIMENTEL*, Li DAI†, Joost PIL‡, Jan TYTGAT‡, Terumi NAKAJIMA§, Gerardo CORZO§‖, Hervé DARBON*[1] and Gilles FERRAT*§

*Architecture et Fonction des Macromolécules Biologiques, UMR 6098, CNRS et Universités d'Aix-Marseille I et II, 31 Chemin Joseph Aiguier, 13402 Marseille Cedex 20, France, †Department of Entomology, University of California, Riverside, Riverside, CA 92521, U.S.A., ‡Laboratory of Toxicology, University of Leuven, E, Van Evenstraat 4, B-3000 Leuven, Belgium, §Suntory Institute for Bioorganic Research, Mishima-Gun, Shimamoto-Cho, Wakayamadai 1-1-1, Osaka 618-8503, Japan, and ‖Department of Molecular Recognition and Structural Biology, Institute of Biotechnology, Av. Universidad, Cuernavaca, Morelos, Mexico

The Om-toxins are short peptides (23–27 amino acids) purified from the venom of the scorpion *Opisthacanthus madagascariensis*. Their pharmacological targets are thought to be potassium channels. Like Csα/β (cystine-stabilized α/β) toxins, the Om-toxins alter the electrophysiological properties of these channels; however, they do not share any sequence similarity with other scorpion toxins. We herein demonstrate by electrophysiological experiments that Om-toxins decrease the amplitude of the K^+ current of the rat channels Kv1.1 and Kv1.2, as well as human Kv1.3. We also determine the solution structure of three of the toxins by use of two-dimensional proton NMR techniques followed by distance geometry and molecular dynamics. The structures of these three peptides display an uncommon fold for ion-channel blockers, Csα/α (cystine-stabilized α-helix–loop–helix), i.e. two α-helices connected by a loop and stabilized by two disulphide bridges. We compare the structures obtained and the dipole moments resulting from the electrostatic anisotropy of these peptides with those of the only other toxin known to share the same fold, namely κ-hefutoxin1.

Key words: cystine-stabilized helix–loop–helix structural motif, NMR, *Opisthacanthus madagascariensis*, potassium channel, scorpion toxin, structure determination.

INTRODUCTION

Numerous small proteins that are natural ligands for ion channels have been described in the literature. Until recently, these toxins were classified into two main families according to their structural motifs. The Csα/β (cystine-stabilized α/β) motif was the first to be described for scorpion toxins that act on potassium and sodium channels [1]. The structure of these toxins consists of a small double- or triple-stranded antiparallel β-sheet linked to a short α-helix by two disulphide bridges. An additional (occasionally two) disulphide bond(s) further stabilizes the motif [2–4]. Members of the second structural family contain the ICK (inhibitor cystine knot) motif, which can be described as a knot of disulphides (two disulphides and part of the backbone of the protein form a ring, and a third disulphide threads through this ring, leading to the definition of the knot) in the core of the protein [5–7]. This knot is closely associated with a double- or triple-stranded antiparallel β-sheet, which is the only regular secondary structure element in these toxins. These toxins act on potassium, sodium and calcium channels [8,9].

We herein report the determination of the solution structure of three Om-toxins, purified from the venom of the scorpion *Opisthacanthus madagascariensis*, using ^{1}H-NMR techniques, thus characterizing a fold only described previously for κ-hefutoxin1 [10], and we discuss the pharmacological properties and selectivity of these peptides towards mammalian potassium channels. It has been found that OmTx2 (toxin 2 from the venom of the scorpion *Opisthacanthus madagascariensis*) alters glucose-induced insulin release from pancreatic islets, while none of the tested peptides exhibited any toxicity towards mice, crayfish or several species of insect (L. Dai, unpublished work). In the present paper, we demonstrate the ability of Om-toxins to bind to Kv1.1, Kv1.2 and Kv1.3 potassium channels.

MATERIALS AND METHODS

Materials

Scorpion venom glands were cut into pieces and extracted with acetonitrile/water (1:1, v/v) in 0.1 % TFA (trifluoroacetic acid). The supernatant was kept at -20 °C until use.

Purification of peptides

The supernatant was applied to a 0.96 mm × 400 mm column containing Sephadex G-25 equilibrated with 50 mM acetic acid, at a flow rate of 0.02 ml/min. The absorbance of the eluent was monitored at 220 nm. Subfractions were checked by MALDI-TOF (matrix-assisted laser-desorption ionization–time-of-flight) MS. Subfraction B was separated further by C_{18} HPLC (Tosoh, TSK gel, ODS 120T, 0.46 cm × 25 cm) at 40 °C with a 40 min linear gradient of 12.5–60 % (v/v) actonitrile/water in 0.1 % TFA. The flow rate was set at 1 ml/min and the absorbance was monitored at 220 nm. Fractions 17, 18, 20 and 27, containing the four peptides, were collected, freeze-dried and purified further by HPLC (TSK gel ODS 120T) with a linear gradient of 12.5–60 % (v/v) acetonitrile in 0.01 M ammonium acetate, pH 5.8, in 40 min.

Amino acid composition and sequencing with MS/MS (tandem MS)

The amino acid composition of each peptide was determined after acid hydrolysis [6 M HCl, 1 % (w/v) phenol] under vacuum at

Abbreviations used: Csα/α, cystine-stabilized α-helix–loop–helix; Csα/β, cystine-stabilized α/β; TFA, trifluoroacetic acid; ICK, inhibitor cystine knot; LC, liquid chromatography; MALDI-TOF, matrix-assisted laser-desorption ionization–time-of-flight; nOe, nuclear Overhauser effect; OmTx1 (etc.), toxin 1 (etc.) from the venom of the scorpion *Opisthacanthus madagascariensis*; R.M.S.D., root mean square deviation.

[1] To whom correspondence should be addressed (email herve@afmb.cnrs-mrs.fr).

The PDB co-ordinate files are available in the Brookhaven Data Bank (PDB codes 1WQC, 1WQD and 1WQE).

© 2005 Biochemical Society

110 °C for 24 h. The dried hydrolysed sample was derivatized with phenyl isothiocyanate and the subsequent phenylthiocarbamyl amino acids were separated at 40 °C on a capillary C_{18} HPLC column (Tosoh, TSK gel, ODS 80T, 0.25 mm × 150 mm), by a linear gradient of 2–70 % solvent B (60 % acetonitrile/water) in solvent A (50 mM sodium acetate) in 20 min. The absorbance was monitored at 254 nm. Amino acid standards derivatized with phenyl isothiocyanate were used for calibration.

The purified peptides were reduced and alkylated by tributylphosphine and 4-vinylpyridine. The alkylated products were desalted by C_{18} HPLC with a 60 min gradient of 0–64 % (v/v) acetonitrile in 0.1 % TFA and monitored by MALDI-TOF MS. Each alkylated peptide was digested with trypsin and applied directly on LC/MS (where LC is liquid chromatography) and LC/MS/MS. To distinguish the isobaric pairs Gln and Lys, the fragment was acetylated in acetic anhydride/acetic acid (1:1, v/v).

Disulphide bridge pattern determination

Each purified peptide was dissolved in 50 μl of 0.1 M ammonium acetate (pH 8.0) and then injected into a V8 protease column for digestion at 37 °C for 30 min. The digested products were washed out and collected. After monitoring by MALDI-TOF MS, the digested products were applied to a trypsin column under the same conditions. The digested products were again monitored by MALDI-TOF MS. Since there are only three possibilities for disulphide bridge formation among the four cysteine residues (first–second and third–fourth; first–third and second–fourth; first–fourth and second–third), we analysed the fragments by MS to elucidate which of these patterns was correct.

Chemical synthesis

Peptides were synthesized using an automated solid-phase peptide synthesizer (433-A; Applied Biosystems), based on the Fmoc (fluoren-9-ylmethoxycarbonyl) strategy. The crude products were dissolved in 0.1 M ammonium acetate buffer, pH 7.7, containing 1 mM GSH and 0.1 mM GSSG at a final concentration of 10 μM and oxidized by exposure to air at room temperature for 24 h. Purification to homogeneity of the oxidized peptides was carried out on a preparative C_{18} reverse-phase HPLC column, using a 30 min linear gradient of 12–42 % (v/v) acetonitrile/water (1:1, v/v) in 0.1 % TFA. The identity of synthetic and natural products was confirmed by MS analysis, C_{18} HPLC co-injection, and amino acid composition analysis.

Expression in *Xenopus* oocytes

Three types of the voltage-gated potassium channels of the shaker (Kv1) family were studied: Kv1.1, Kv1.2 (both from rat) and Kv1.3 (from human).

Plasmids containing Kv1.1 were linearized with PstI (New England Biolabs) 3′ to the 3′ non-translated β-globin sequence in a custom-made high expression vector for oocytes, pGEM-HE [11], and then transcribed using an mMESSAGE mMachine T7 transcription kit (Ambion). The cDNA encoding Kv1.2 in its original vector, pAKS2, was first subcloned into pGEM-HE [11]. The insert was released by double restriction digestion with BglII and EcoRI, and ligated into the BamHI and EcoRI sites of pGEM-HE. For *in vitro* transcription, the cDNA was linearized with SphI and transcribed using a large-scale T7 mMESSAGE mMachine transcription kit (Ambion). The plasmid pCI.neo, containing the gene for Kv1.3, was linearized with NotI (Promega) and transcribed as for Kv1.2.

Stage V–VI *Xenopus laevis* oocytes were harvested by partial ovariectomy under anaesthesia (3-aminobenzoic acid ethyl ester methanesulphonate salt, 0.5 g/l; Sigma). Anaesthetized animals were kept on ice during dissection. The oocytes were defolliculated by treatment with 2 mg/ml collagenase (Sigma) in Ca^{2+}-free ND-96 solution (96 mM NaCl, 2 mM KCl, 1 mM $MgCl_2$, 5 mM Hepes, adjusted to pH 7.5). Between 1 and 24 h after defolliculation, oocytes were injected with 10 nl of 5–100 ng/μl RNA. The oocytes were then incubated in ND-96 solution (supplemented with 50 mg/ml gentamycin sulphate) at 16 °C for 1 day.

Electrophysiological measurements

Two-electrode voltage-clamp recording was performed at room temperature using a GeneClamp 500 amplifier (Axon Instruments) controlled by a pClamp data acquisition system (Axon Instruments). Whole-cell currents from oocytes were recorded 1 day after injection. Voltage and current electrodes were filled with 3 M KCl. The resistances of both electrodes was kept as low as possible (< 0.5 MΩ). The bath solution composition was (in mM): NaCl 96, KCl 2, $CaCl_2$ 1.8, $MgCl_2$ 2, Hepes 5 (pH 7.4). Using a four-pole low-pass Bessel filter, currents were filtered at 1 kHz and sampled at 2 kHz. Current traces were evoked in an oocyte expressing Kv channels by depolarization to 0 mV from a potential of -90 mV.

NMR sample preparation

Purified OmTx1, OmTx2 and OmTx3 (molecular mass 2984 Da, 3148 Da and 2518 Da respectively) were each solubilized in 500 μl of a mixture of H_2O and ^2H_2O (9:1, v/v), at a final protein concentration of 2.0 mM for each sample. Amide proton exchange rates were determined after freeze-drying of these samples and dissolution in 100 % ^2H_2O.

NMR experiments

All ^{1}H-NMR spectra were recorded on a Bruker DRX500 spectrometer equipped with a HCN probe and self-shielded triple axis gradients. The experiments were performed at two different temperatures, 283 K and 290 K, in order to solve assignment ambiguities. Two-dimensional spectra were acquired using the States-TPPI method [12] to achieve F1 quadrature detection [13]. Water suppression was obtained either by using presaturation during the 1.3 s relaxation delay and during the mixing time (120 ms) for NOESY spectra, or with a watergate 3-9-19 pulse train [14] using a gradient at the magic angle obtained by applying simultaneous x, y and z gradients prior to detection. TOCSY spectra were obtained with a spin-lock time of 80 ms and a spin locking field strength of 8 kHz. The individual amide proton exchange rates were determined by recording a series of four NOESY spectra (each experiment was 10 h long) at 283 K using the ^2H_2O sample. Amide protons still giving rise to nOe (nuclear Overhauser effect) correlations after 40 h of exchange were considered as slowly exchanging, and therefore engaged in a hydrogen bond.

Spectrum analysis and experimental restraints

Spectrum analysis was performed using the graphics software XEASY [15]; the identification of amino acid spin systems and sequential assignments were performed using the standard strategy described by Wüthrich [16] and used regularly by our group [17–19]. The comparative analysis of COSY and TOCSY spectra recorded in water allowed us to determine the spin system signatures of the protein. The spin systems were then connected sequentially using the NOESY spectra.

The integration of nOe data was done by measuring the peak volumes. These volumes were then translated into upper limit

© 2005 Biochemical Society

distances by the CALIBA routine of the DIANA software. The lower limit was systematically set at 0.18 nm. The Φ torsion angle constraints were estimated from the $^3J_{HN-H\alpha}$ coupling constants measured on a COSY spectrum, with 8192 data points in the acquisition dimension, as described previously [13]. These Φ angles were restrained to $-120 \pm 40°$ for $^3J_{HN-H\alpha} \geqslant 8$ Hz and to $-65 \pm 25°$ for $^3J_{HN-H\alpha} \leqslant 6$ Hz. No angle constraint was assigned to $^3J_{HN-H\alpha} = 7$ Hz, a value considered as ambiguous. These angles were used as constraints in the final runs of DIANA calculations and during energy minimization. Determination of the amide proton exchange rates led us to identify protons involved in hydrogen bonding. Their oxygen partners were then identified by visual inspection of the preliminary calculated structures.

Structure calculation

Distance geometry calculations were performed with the variable target function program DIANA 2.8. A preliminary set of 1000 structures was initiated including only intra-residual and sequential upper limit distances. From these, the 500 best (i.e. with the lowest residual nOe violations) were kept for a second round, including medium-range distances, and then the 250 best for the third round, with the whole set of upper-limit restraints. The 125 best preliminary structures were kept for the fourth round of calculation, in which experimentally determined disulphide bridges (i.e. $d_{S\gamma,S\gamma}$ 0.21 nm; $d_{C\beta,S\gamma}$ and $d_{S\gamma,C\beta}$ 0.31 nm) as well as dihedral constraints were added. Finally, based on the 100 best solutions, a REDAC strategy was used in order to refine the 50 best solutions by including the additional distance restraints from hydrogen bonds.

To remove residual poor van der Waals contacts, these 50 structures were then refined by restrained molecular dynamics annealing, slow cooling, and energy minimization using CNS [20] (parameter file: protein-allhdg).

Visual analysis of the final structures was done using TURBO [21] and Molmol [22] graphics software, and the geometric quality of the obtained structures was assessed using PROCHECK-NMR [23]. The representation of the structure was performed using TURBO and Molscript-RASTER3D [24,25].

Electrostatic calculations

The electrostatic potentials and dipole moments of the toxins were calculated using GRASP software [26] running on a Silicon Graphics Workstation. This calculation includes all ionizable groups, based on the Amber force field of the residues. The potential maps were calculated with a simplified Poisson–Boltzmann solver [26,27].

RESULTS AND DISCUSSION

Purification and primary structure determination

When screening the scorpion crude venom by LC/MS (results not shown), four peptides with a molecular mass of approx. 3 kDa were identified as the main components. In order to purify the four peptides, the crude venom extract was first separated by gel filtration. The subfraction that contained the four peptides was further separated by reverse-phase HPLC under the conditions described above. Fractions containing OmTx1, OmTx2, OmTx3 and OmTx4 were collected and the peptides were subsequently purified to homogeneity by reverse-phase HPLC (Figure 1). Amino acid composition analysis of the pure peptides is given in Table 1.

The four peptides were reduced and alkylated with 4-vinylpyridine. The alkylated peptides were desalted by reverse-phase HPLC and checked by MALDI-TOF MS, and the mass difference between the alkylated and original peptides demonstrated that all the peptides contain four cysteine residues, which are suggested to form two disulphide bridges.

The alkylated peptides were then digested with trypsin and applied to LC/MS and LC/MS/MS (Figure 2). Peptide OmTx2 gave four Lys–Xaa fragments, and LC/MS/MS results showed that fragments 2–4 overlapped due to incomplete digestion. Combining the amino acid composition results and MS/MS results, position 8 in fragment 1 should be Leu. Lys was determined to be the C-terminal residue in both fragment 1 and fragment 2. Positions 9 and 10 should both be Gln. The amino acid sequencing results for OmTx1 and OmTx4 showed strikingly high identity with OmTx2, and the only difference was at the C-terminus.

Peptide OmTx3 gave two Lys–Xaa fragments, and each fragment was analysed by MS/MS. However, we could not determine which fragment was N-terminal or C-terminal, because both fragments had Gln/Lys at the C-terminus. To distinguish the two

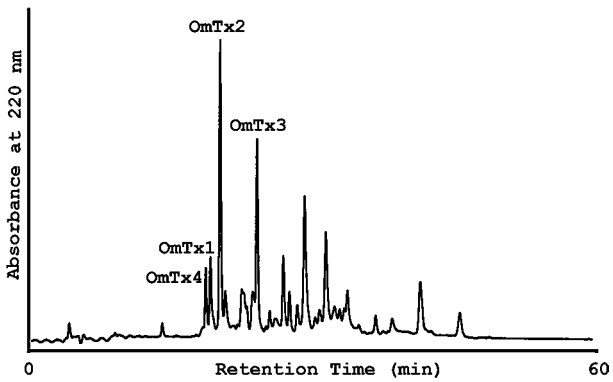

Figure 1 Purification four peptides from the venom of the scorpion *Opisthacanthus madagascariensis*

The subfraction containing the Om-toxins was separated by reverse-phase HPLC (TSK gel ODS 120-T column; 0.46 cm × 25 cm) with a 40 min linear gradient of 12.5–60 % (v/v) acetonitrile/water (1:1, v/v) in 0.1 % TFA. The fractions containing the four peptides OmTx1, OmTx2, OmTx3 and OmTx4 were collected, and the peptides were lyophilized and further purified by HPLC on a TSK ODS 120T gel with a linear gradient of 12.5–60 % acetonitrile in 0.01 M ammonium acetate, pH 5.8, in 40 min.

Table 1 Amino acid composition of the four peptides

Values in parentheses are rounded up or down to the nearest whole number.

	Amino acid composition (residues/mol of peptide)			
Residue	OmTx1	OmTx2	OmTx3	OmTx4
Asx	1.6 (2)	1.7 (2)	2.6 (3)	1.6 (2)
Glx	6.6 (7)	6.6 (7)	5.5 (6)	5.5 (6)
Ser	0	0	0	0
Gly	1.0 (1)	1.2 (1)	1.2 (1)	1.1 (1)
His	2.0 (2)	2.1 (2)	0.9 (1)	2.1 (2)
Thr	0	0	0.8 (1)	0
Ala	1.1 (1)	1.1 (1)	2.1 (2)	1.2 (1)
Pro	2.1 (2)	2.0 (2)	1.1 (1)	2.1 (2)
Arg	0	0	0	0
Tyr	0.7 (1)	1.8 (2)	0	0.7 (1)
Val	2.9 (3)	2.8 (3)	2.0 (2)	2.0 (2)
Met	0	0	0	0
Cys	–	–	–	–
Ile	0	0	1.8 (1)	0
Leu	1.2 (1)	1.1 (1)	0	1.2 (1)
Lys	1.7 (2)	1.8 (2)	0.8 (1)	1.6 (2)
Total	26	27	23	24

© 2005 Biochemical Society

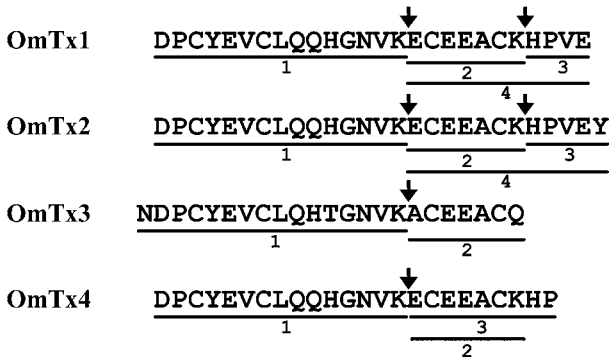

Figure 2 Amino acid sequence determination of OmTx1, OmTx2, OmTx3 and OmTx4

The alkylated peptides were digested with trypsin and subjected to LC/MS and LC/MS/MS analysis. The arrows show cleavage sites.

residues, ladder sequencing (digestion by C-terminal carboxypeptidase) was performed with alkylated OmTx3. The results (the C-terminal three residues were Ala-Cys-Lys/Gln) showed that fragment 2 is the C-terminal fragment. Thus position 16 in fragment 1 should be Lys, and position 10 in fragment 1 and position 7 in fragment 2 should be Gln. The amino acid sequences of the four peptides were determined as shown in Figure 2. All peptides are rich in acidic residues (Glu and Asp) and their calculated pI values are below 5. This is quite different from other known scorpion neurotoxins, which contain three or four S–S bonds and are rich in basic residues.

The four peptides were then synthesized by chemical solid-phase synthesis methods, and showed HPLC retention times identical with the native peptides.

Disulphide bridge pattern determination

Enzyme digestion and MALDI-TOF MS were used to identify the disulphide bridge pattern. Since there were only three connecting possibilities among the four cysteine residues (first–second and third–fourth; first–third and second–fourth; first–fourth and second–third), we analysed the fragments by MS to elucidate which of these patterns was correct. The results showed that the first and fourth cysteine residues, and the second and third cysteines, were connected by disulphide bridges in each of the three peptides (results not shown).

Electrophysiology

OmTx1, OmTx2 and OmTx3 were screened for K^+ channel blocking activity in *Xenopus laevis* oocytes expressing a single type of voltage-gated K^+ channel, namely Kv1.1, Kv1.2 or Kv1.3 (Figure 3). The application of 500 μM OmTx1 produced 17 %, 12 % and 24 % blockade of Kv1.1, Kv1.2 and Kv1.3 channels respectively. The addition of 500 μM OmTx2 resulted in a small blockade of 8 % and 10 % for Kv1.1 and Kv1.2 respectively, whereas a blockade of 36 % was observed for Kv1.3 channels. The blockade induced by 500 μM OmTx3 was 33 % and 8 % for Kv1.1 and Kv1.2 channels respectively, while for Kv1.3 channels a 70 % blockade was observed. Data are means of at least four experiments in all cases.

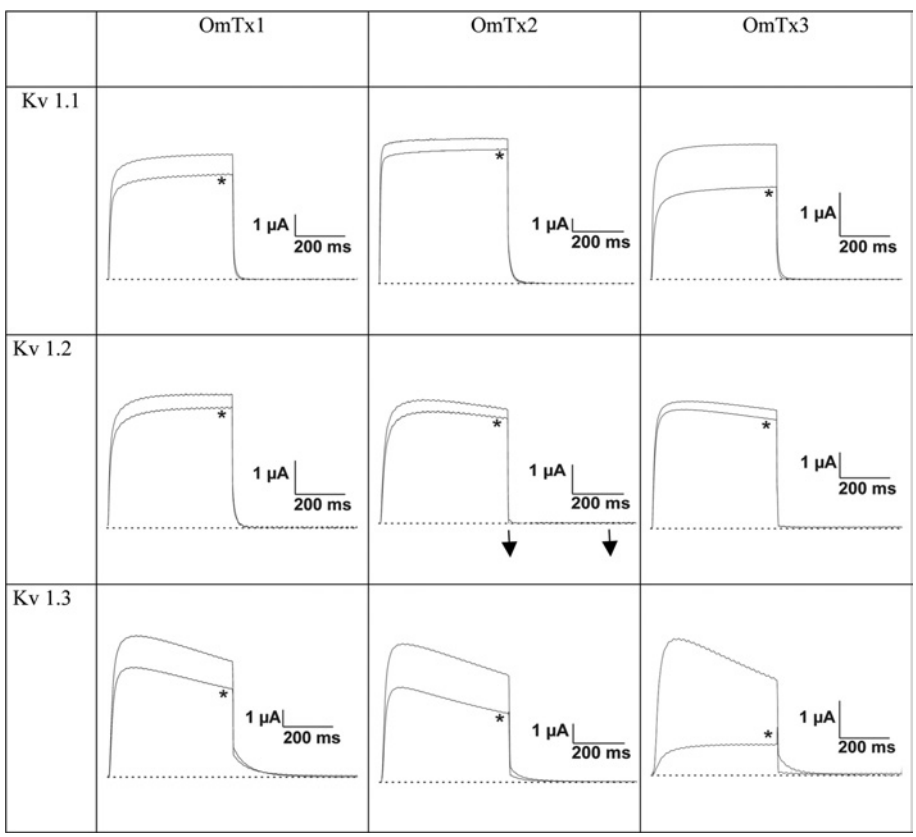

Figure 3 Effects of OmTx1, OmTx2 and OmTx3 on Kv1.1, Kv1.2 and Kv1.3 channels expressed in *Xenopus laevis* oocytes

Control conditions are compared with the presence of the toxin (500 μM; indicated by *). See the text for details.

© 2005 Biochemical Society

Table 2 Chemical shifts of OmTx1 (A), OmTx2 (B) and OmTx3 (C) at 283 K

*Resonances that cannot be observed.

(A) OmTx1

Residue	Chemical shift (p.p.m.) HN	Hα	Hβ	Others
D-1	*	4.37	2.68,*	
P-2		4.28	2.18,*	Hγ 1.88, 1.82; Hδ 3.59
C-3	8.11	3.90	3.07, 2.97	
Y-4	8.25	3.71	2.86, 2.76	Hδ 6.70; Qε 6.55
E-5	7.66	3.67	1.91,*	Hγ 2.34
V-6	7.85	3.44	1.84	Hγ1 0.78; Hγ2 0.65
C-7	7.76	4.10	2.91, 2.8	
L-8	8.08	3.61	1.22, 1.34	Hγ 1.18; Hδ 0.45
Q-9	7.61	3.81	1.97,*	Hγ 2.32, 2.19; Hε2 0.23, 6.60
Q-10	7.47	3.93	1.74,*	Hγ 2.29, 2.09; Hε2 7.19, 6.61
H-11	8.04	4.34	3.17, 3.06	Hδ2 7.16; Hε1 8.40
G-12	8.03	3.58, 3.89		
N-13	*	4.59	2.68, 2.51	Hδ2 7.59, 6.77
V-14	8.16	3.38	1.76	Hγ 0.84, 0.71
K-15	8.09	3.81	1.47, 1.30	Hγ 1.17; Hδ 1.58; Hε 3.81; Hζ 7.35
E-16	7.95	3.81	1.79,*	Hγ 2.25, 2.11
C-17	8.08	4.33	2.77, 2.67	
E-18	8.67	3.75	1.73, 2.05	Hγ 1.94, 2.22
E-19	7.64	3.87	1.97,*	H 2.40, 2.34
A-20	7.91	3.99	1.32,*	
C-21	7.31	4.49	3.12, 2.83	
K-22	7.46	3.97	1.63, 1.57	Hγ 1.23, 1.17; Hδ 1.45; Hε 2.74; Hζ 7.36
H-23	8.19	4.79	3.00, 2.89	Hδ2 7.07; Hε1 8.39
P-24		4.29	2.07, 1.69	Hγ 1.78; Hδ 3.47, 3.33
V-25	8.21	3.86	1.84	Hγ 0.78
E-26	8.21	4.15	1.96, 1.74	Hγ 2.21

(B) OmTx2

Residue	Chemical shift (p.p.m.) HN	Hα	Hβ	Others
D-1	*	*	2.18,*	
P-2		4.36	2.67,*	Hγ 1.82; Hδ 3.60
C-3	8.11	3.90	3.08, 2.97	
Y-4	8.24	3.70	2.86, 2.76	Hδ 6.70; Hε 6.56
E-5	7.67	3.67	1.91,*	Hγ 2.34
V-6	7.85	3.44	1.69	Hγ1 0.78; Hγ2 0.65
C-7	7.76	4.09	2.89, 2.82	
L-8	8.08	3.61	1.35, 1.19	Hγ 1.180; Hδ 0.44
Q-9	7.61	3.81	1.98,*	Hγ 2.32, 2.20; Hε2 7.19, 6.61
Q-10	7.47	3.94	1.75,*	Hγ 2.29, 2.09
H-11	8.04	4.35	3.17, 3.06	Hδ 7.16
G-12	8.02	3.58, 3.91		
N-13	8.67	*	2.68, 2.51	Hδ2 7.59, 6.77
V-14	8.16	3.38	1.76	Hγ1 0.84; Hγ2 0.71
K-15	8.09	3.81	1.90, 1.62	Hγ 1.30, 1.17; Hδ 1.48; Hε 2.76; Hζ 7.36
E-16	7.95	3.82	1.79,*	Hγ 2.25, 2.12
C-17	8.09	3.83	2.76,*	
E-18	8.67	3.75	2.05,*	Hγ 1.73
E-19	7.63	3.86	1.94,*	Hγ 2.38
A-20	7.92	3.99	1.33,*	
C-21	7.31	4.47	3.12, 2.83	
K-22	7.44	3.97	1.63,*	Hγ 1.25, 1.16; Hδ 1.46; Hε 2.75
H-23	8.16	4.81	2.99, 2.89	Hδ 7.07
P-24		4.28	2.08, 1.68	Hγ 1.78; Hδ 3.48, 3.34
V-25	8.12	3.78	1.72	Hγ1 0.69; Hγ2 0.57
E-26	8.11	4.14	1.81, 1.65	Hγ 2.17
Y-27	7.98	4.30	2.90, 2.68	Hδ 6.89

(C) OmTx3

Residue	Chemical shift (p.p.m.) HN	Hα	Hβ	Others
N-1	*	4.16	2.70,*	Hδ 6.76, 7.41
D-2	8.51	4.80	2.81,*	
P-3		4.14	1.76, 2.15	Hγ 1.77, 1.90; Hδ 3.61,*
C-4	8.04	3.90	2.93, 2.96	
E-5	8.05	3.48	1.87,*	Hγ 2.03, 2.19
E-6	8.12	3.78	1.90,*	Hγ 2.27,*
V-7	7.91	3.52	1.84	Hγ1 0.66; Hγ2 0.81
C-8	7.62	4.23	2.93,*	
I-9	8.74	3.28	1.68	Hγ2 0.54; Hγ 1.47, 1.68; Hδ1 0.69
Q-10	7.91	3.83	1.95,*	Hγ 2.14, 2.29; Hε2 7.22, 6.59
H-11	7.66	4.51	3.15,*	Hδ2 7.33; Hε1 7.99
T-12	8.13	4.35	4.07	Hγ2 1.09
G-13	8.61	3.91, 3.66		
D-14	7.69	4.65	2.93, 2.38	Hγ1 0.62; Hγ2 0.79
V-15	8.09	3.12	1.75	
K-16	8.32	3.79	1.61,*	Hγ 1.16, 1.26; Hδ 1.47; Hε 2.75
A-17	7.34	3.89	1.10,*	
C-18	7.89	4.25	2.67, 2.79	
E-19	8.36	3.73	1.85, 2.10	Hγ 2.10, 2.45
E-20	7.59	3.85	1.92,*	Hγ 2.29, 2.39
A-21	7.78	4.02	1.29,*	
C-22	7.36	4.45	2.77, 3.09	
Q-23	7.46	4.09	1.89,*	Hγ 2.00, 2.24; Hε2 6.65, 7.34

NMR assignment and secondary structures

The spin systems were identified on the basis of both COSY and TOCSY spectra recorded at 283 K and 290 K. Sequential assignment was obtained by the now standard method first described by Wüthrich [16] and applied successfully to various scorpion toxins [28]. The use of two temperatures allowed us to resolve overlapping signals in the fingerprint region. Intraresidual HN–Hα cross-peaks were thus unambiguously assigned. At the end of the sequential assignment procedure, almost all protons were identified and their resonance frequencies assigned (Table 2). The repartition of the HN_i/HN_{i+1}, $H\alpha_i/HN_{i+3}$ and $H\alpha_i/HN_{i+4}$ nOe correlations, together with small coupling constants, indicated that the toxins are mainly organized in a helix beside a short loop region characterized by the presence of $H\alpha_i/HN_{i+1}$ and the absence of medium-range correlations (Figures 4B–4D).

The sequence of OmTx1 is similar to that of OmTx2, except that OmTx2 posseses an additional Tyr residue at its C-terminus (Figure 4A). Analysis of the OmTx1 and OmTx2 spectra revealed that their amide proton chemical shifts are nearly identical from residue Cys-3 to residue His-23 (Figure 5), with variation in the chemical shifts of less than 0.03 p.p.m. As the chemical shift of a given proton is a function of the nature of the proton and of its chemical and electromagnetic neighbourhood, these small variations could be due to a difference in the conformation of the C-termini of OmTx1 and OmTx2, as well as to the presence of the Tyr-27 in OmTx2. Since the sequence of OmTx3 presents less similarity to the sequences of the other Om-toxins, we observe more differences in the chemical shifts (Figures 4A and 5).

Structure calculations

We collected 339, 336 and 281 nOes for OmTx1, OmTx2 and OmTx3 respectively from the different NOESY spectra. These nOes were converted into distance restraints, and 254, 249 and 216 of these were meaningful for determining the structures of the Om-toxins. The restraints were distributed as follow: 109, 102 and 89 intra-residual restraints; 82, 91 and 69 sequential restraints; 43, 43 and 43 medium-range restraints; and 20, 13 and 15 long-range restraints, for OmTx1, OmTx2 and OmTx3 respectively.

© 2005 Biochemical Society

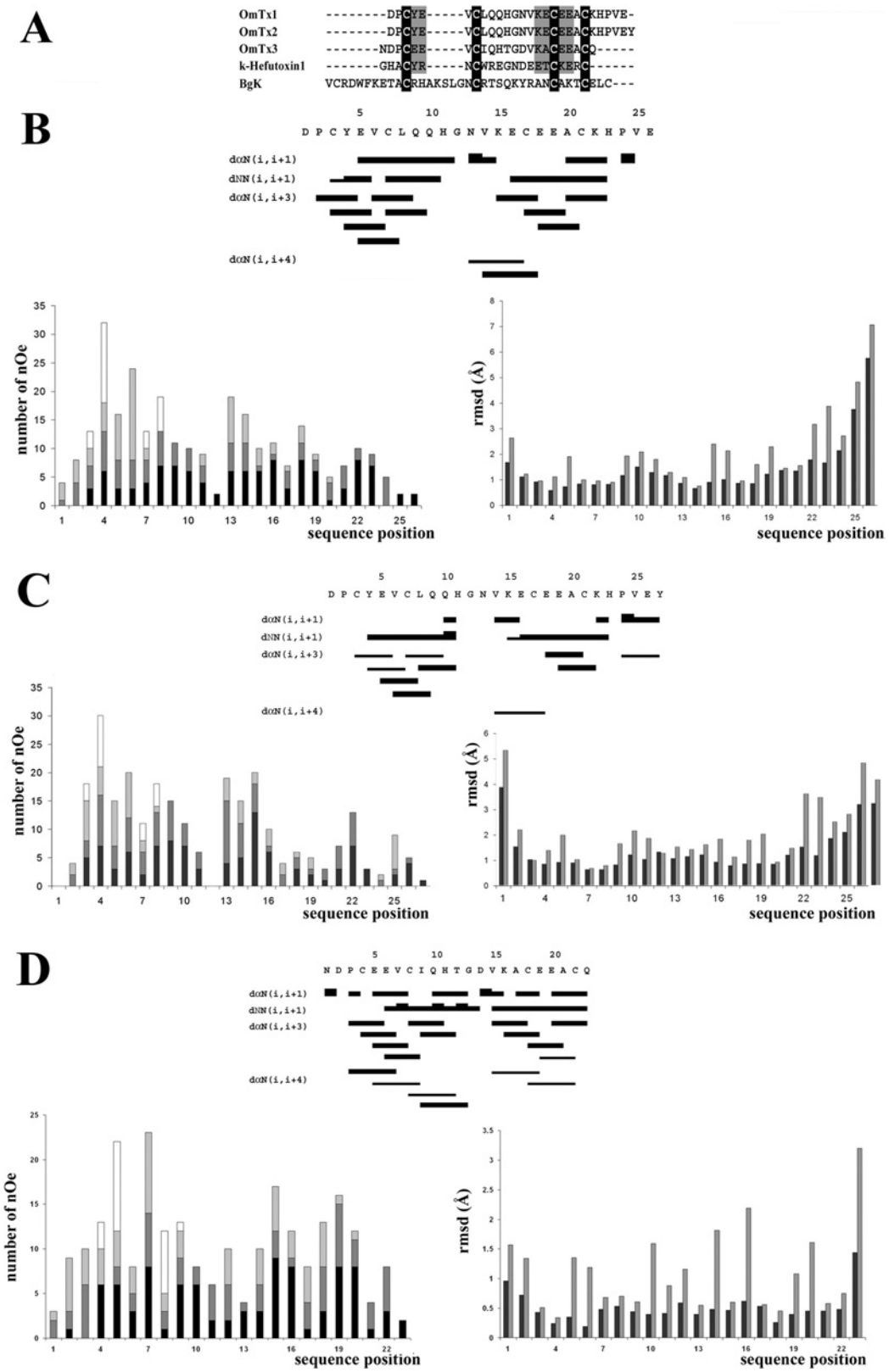

Figure 4 Sequence alignment of Om-toxins with related toxins (A), and nOe statistics for OmTx1 (B), OmTx2 (C) and OmTx3 (D)

(**A**) Sequence alignment of the three Om-toxins with κ-hefutoxin1 isolated from the scorpion *Heterometrus fulvipes* and BgK toxin from the sea anemone *Bunodosoma granulifera*. Cysteine residues are highlighted in black, and conserved residues are highlighted in grey. (**B**) Upper panel: sequence of OmTx1 and sequential assignment. Collected nOes are classified into weak, medium and strong, which are indicated by thin, medium and thick lines respectively. Lower panels: nOe and R.M.S.D. distribution for OmTx1. Intraresidue nOes are designated by black bars, sequential nOes by dark grey bars, medium nOes by light grey bars and long-range nOes by white bars. R.M.S.D. values for backbone and all heavy atoms are indicated by black and grey bars respectively. (**C**) As in (**B**), for OmTx2 (**C**) and OmTx3 (**D**).

© 2005 Biochemical Society

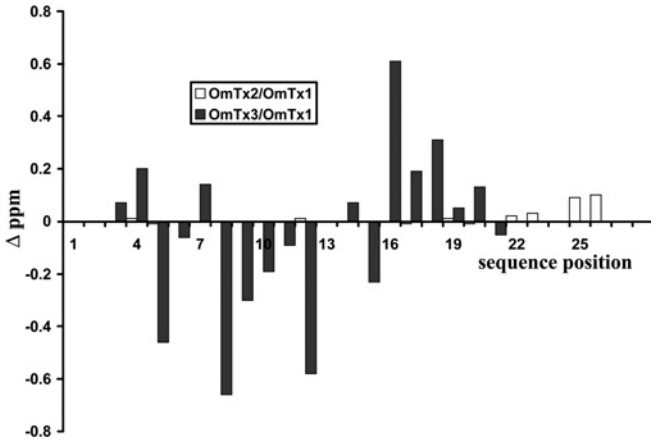

Figure 5 Chemical shift variations in relation to sequence for OmTx2 compared with OmTx1 (□) and for OmTx3 compared with OmTx1 (■)

Table 3 Structural data for the three Om-toxins

Cdih, constrained dihedral angle. Energy values are given in kcal/mol; 1 kcal = 4.184 kJ.

Parameter	OmTx1	OmTx2	OmTx3
RMSD (Å)			
Backbone (all residues)	1.86 ± 0.65	1.71 ± 0.51	0.60 ± 0.22
Backbone (residues 2–23/2–23/1–23)	0.71 ± 0.22	0.76 ± 0.19	0.60 ± 0.22
All heavy atoms	2.73 ± 0.64	2.70 ± 0.62	1.45 ± 0.26
All heavy atoms (residues 2–23/2–23/1–23)	1.69 ± 0.28	1.71 ± 0.34	1.45 ± 0.26
Energy (kcal/mol)			
Total	56.1970	47.1435	45.4989
Bonds	3.3090	2.4059	2.7842
Angles	21.8483	22.9904	18.2006
Impropers	1.7721	1. 6504	1.0991
van der Waals (repel)	11.7589	12.3917	10.8586
nOe	17.1355	7.6862	12.5407
Cdih	0.3733	0.0188	0.0158
R.M.S.D.			
Bonds (Å)	0.0029	0.0024	0.0029
Angles (°)	0.4455	0.4456	0. 4511
Impropers (°)	0.2378	0.2194	0.2139
Dihedral (°)	31.1720	30.8995	30.6461
nOe (Å)	0.0282	0.0193	0.0261
Cdih (°)	0.4503	0.0844	0.0897

The distribution of these nOes along the sequence is shown in Figures 4(A)–4(C). In addition, 26, 16 and 20 hydrogen bond restraints and 12, 13 and 11 dihedral angle constraints respectively derived from proton exchange and coupling constants were included, as well as six distance restraints, for each structure, derived from the experimentally characterized disulphide bridges. Altogether, the final experimental set led to an average of 11.5, 10.5 and 11 constraints per residue for OmTx1, OmTx2 and OmTx3 respectively.

The distance geometry calculations using the whole set of restraints in DIANA [29], followed by energy minimization using the CNS program, gave a single family of 30 solutions for each of the three Om-toxins. A summary of the structural statistics and the R.M.S.D. (root mean square deviation) values calculated for the well defined regions are given in Table 3. The discrepancy between R.M.S.D. values calculated for the whole sequences and for all residues except the N- and C-termini indicates poor resolution of these residues. This is confirmed by the individual R.M.S.D. values (Figure 4). This poor resolution, for the C-terminal part of the toxin in particular, is due to the lack of structural restraints and may arise from a higher mobility of these residues in solution (Figure 6A).

All structures have good non-bonded contacts and good covalent geometry, as shown by low values of CNS energy terms and low R.M.S.D. values for bond lengths, valence angles and improper dihedral angles (Table 3). The correlation with the experimental data shows no nOe-derived distance violations greater than 0.2 Å.

The analysis of the Ramachandran plots for the ensemble of the 30 calculated structures for each Om-toxin revealed that 79.8 %, 59.4 % and 80.5 % of the residues are in the most favoured region; 13.5 %, 38.0 % and 19.3 % are in the additionally allowed region; 6.7 %, 2.4 % and 0.2 % are in the generously allowed region; and 0 %, 0.2 % and 0 % are in the disallowed region (PROCHECK software nomenclature) for OmTx1, OmTx2 and OmTx3 respectively (results not shown).

Structure of Om-toxins, and comparison with other related toxins

Figure 6 shows the representation of the best superimposition of the backbone traces of the 30 structures for each of the three Om-toxins. The good convergence of the calculated solutions allows us to describe the three-dimensional structures of OmTx1, OmTx2 and OmTx3 (PDB codes 1WQC, 1WQD and 1WQE respectively). The common motif can be described as follows: two helical structures (Pro-2–Gln-9 and Val-14–Cys-21 for OmTx1 and OmTx2; Pro-3–Gln-10 and Val-15–Cys-22 for OmTx3) stabilized by two disulphide bridges (Cys-3–Cys-21 and Cys-7–Cys-17 for both OmTx1 and OmTx2; Cys-4–Cys-22 and Cys-8–Cys-18 for OmTx3). All helices are classified as classical α-helices in view of the existence of typical $H\alpha_i/HN_{i+3}$ and $H\alpha_i/HN_{i+4}$ nOe correlations, together with the presence of hydrogen bonds (NH_i–CO_{i+4}). In each of the three molecules, a four-residue loop links the two helices, although it cannot be classified as a β-turn. These toxins are therefore classified into the Csα/α (cystine-stabilized helix–loop–helix) fold family.

Within this constant fold, some differences arise. The solution structure of OmTx2 shows that the N-terminus is less well defined, and this blurred definition is due to the lack of restraints in this region, which might arise from intrinsic mobility. On the other hand, the family of solution structures of OmTx3 presents two conformations in the neighbourhood of residues 7 and 8, due to the isomerization of the second disulphide bridge involving Cys-8 and Cys-18. The two subfamilies are, however, both in complete agreement with all the applied restraints.

A helix–loop–helix fold is very unusual in the scorpion toxin family: the only other toxin described so far that has the same fold is κ-hefutoxin1 [10], a toxin active on the same channels as Om-toxins, i.e. the Kv1.x channels (Figure 6B). However, κ-hefutoxin1 is not similar in sequence to the Om-toxins, with the exception of cysteine residues and one tyrosine and one glutamic acid (Figure 4A). The helix–loop–helix backbone (Cys-4–Cys-22) of κ-hefutoxin1 matches the helix–loop–helix backbone (Cys-3–Cys-21 or Cys-4–Cys-22) of the Om-toxins, with an R.M.S.D. calculated on backbone atoms of 1.62 Å, 1.40 Å and 1.23 Å for OmTx1, OmTx2 and OmTx3 respectively. However, the loop connecting the two helices of κ-hefutoxin1 has been classified as a β-turn [10].

The only other channel blockers that fold in helical structures are the BgK and ShK toxins from sea anemones (PDB codes 1BGK and 1ROO respectively). However, the Om-toxins cannot

© 2005 Biochemical Society

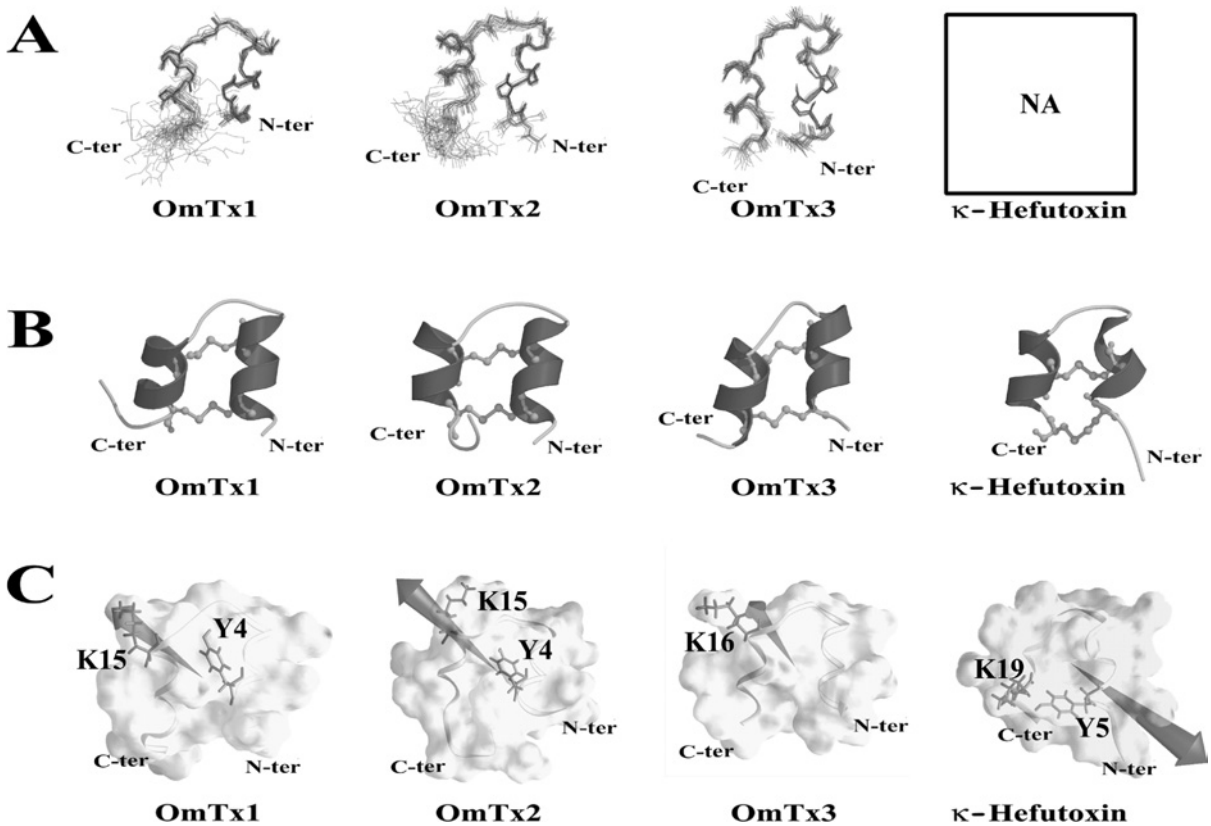

Figure 6 Three-dimensional structure of Om-toxins and κ-hefutoxin, and their dipole moment

(**A**) Stereopair views of the best 30 solution structures [backbone (N, Ca, C)] of the molecules OmTx1, OmTx2 and OmTx3. κ-Hefutoxin structure is not available (NA). (**B**) Molscript representations of OmTx1, OmTx2, OmTx3 and κ-hefutoxin. (**C**) GRASP representations of OmTx1, OmTx2, OmTx3 and κ-hefutoxin. The dipole moments are indicated by the arrows. The surface and the backbone of the toxins are represented.

be strictly classified in the same fold family as BgK and ShK, because the relative orientations of the helices are different (perpendicular to each other for BgK and ShK, compared with antiparallel for the Om-toxins). Although this fold is unusual in the scorpion toxin family, it is found in other proteins, e.g. the viscotoxins VA2 and VB (PDB id 1JMN and 1JMP respectively) produced by mistletoe possess two α-helices linked by a disulphide bridge and connected by a small loop. However, this toxin does not act on any ion channel, but interacts directly with cell membranes. The plant toxins β-purothionin and hellethionin (PDB id 1BHP and 1NBL respectively) fold in the same way as the viscotoxins. The heat-stable enterotoxin B (PDB id 1EHS) from *Escherichia coli* folds around a helix–loop–helix pattern, but the loop between the two helices is much longer compared with the Om-toxins.

Thus it is possible that the Om-toxins and κ-hefutoxin1 have a common genetic origin. Moreover, structural similarity often provides evidence to support a divergent evolutionary mechanism. Zhu et al. [30] studied the evolutionary origin of the ICK peptides, and came to the conclusion that divergent as well as convergent evolution has taken place in the ICK family. The cysteine-rich helix–loop–helix peptides might follow the same evolutionary rules, as they have very different functions.

As toxins can perform a variety of pharmacological functions, careful analysis of the molecular surface of these proteins and delineation of a putative functional surface is of utmost importance for understanding how subtle variations in the primary structure influence the spatial structure of the toxin and hence define a specific pharmacology. With that aim, our group has developed a predictive method to determine the surface of interaction, based on the orientation of the molecular dipole moment which reveals the electrostatic anisotropy of peptides. The molecular surface through which the dipole emerges is hypothesized to be involved in the interaction with the receptor site of the toxin [19,31]. This prediction method appears to fit for toxins acting by pore occlusion, for which structure–activity data based on site-directed mutagenesis are available. The three Om-toxins are rich in acidic residues, an uncommon feature for scorpion toxins, which are generally basic peptides. Applied to the Om-toxins, the analysis of charge distribution indicates a large acidic surface disrupted locally by basic residues. The resulting anisotropy can be represented by an arrow starting from the centre of mass of the molecule and going from the acidic surface towards the basic surface.

The dipole moment calculated on the Om-toxin structures emerges through the C-terminus of the first helix, near to residue Lys-15 for OmTx1 and OmTx2 and the analogous Lys-16 for OmTx3 (Figure 6C). We first assumed that Lys-15 and Tyr-4 of OmTx1 and OmTx2 might be the two components of the typical dyad of the pore blocker [1]: the aromatic residue of the dyad is located in the first helix, and the basic residue is located in the second helix. However, this dyad is not present in OmTx3, due to the lack of the aromatic residue on the first helix, and it turns out that this toxin is the most active of the Om-toxins. This fact reinforces a new proposal according to which the aromatic residue is not crucial for interaction [32]. The dipole moment orientation and the presence of the dyad in two of the Om-toxins are in accordance with the hypothesis that the Om-toxins act as pore blockers.

© 2005 Biochemical Society

Alanine scanning performed on κ-hefutoxin1 has shown that two residues are crucial for channel inhibition, i.e. Lys-19 and Tyr-5. These residues are thought to form a dyad, as already described for Csα/β potassium channel blockers [1]. This toxin has been described as both a gating modifier and a pore blocker, while having partially the same binding pocket as AgTx2 [10]. When applied to the averaged structure of κ-hefutoxin1, the dipole moment does not emerge through Lys-19 of the toxin, but near to the N-terminus, close to the other crucial residue, i.e. Tyr-5. This discrepancy could be explained by a somewhat different mode of action: Om-toxins are proposed to be pore blockers, whereas κ-hefutoxin1 may interact with the outer vestibule of the channel, while having a gating modifier behaviour. In a case such as this, it is possible that both the orientation force of the electrostatic anisotropy and an incompletely interacting surface, i.e. lack of additional residues that are responsible for the high affinity of the classical pore blockers [4], are not sufficient to make those toxins strong channel inhibitors.

B. C. is supported by the Ministère de l'Éducation Nationale, de l'Enseignement Supérieur et de la Recherche (France). G. F. is the recipient of a post-doctoral grant from SUNBOR (Suntory Institute for Bioorganic Research).

REFERENCES

1 Bontems, F., Roumestand, C., Gilquin, B. and Toma, F. (1991) Refined structure of charybdotoxin: common motifs in scorpion toxins and insect defensins. Science **254**, 1521–1523

2 Blanc, E., Romi-Lebrun, R., Bornet, O., Nakajima, T. and Darbon, H. (1998) Solution structure of two new toxins from the venom of the Chinese scorpion *Buthus martensi* Karsch blockers of potassium channels. Biochemistry **37**, 12412–12418

3 Fajloun, Z., Ferrat, G., Carlier, E., Fathallah, M., Lecomte, C., Sandoz, G., di Luccio, E., Mabrouk, K., Legros, C., Darbon, H. et al. (2000) Synthesis, 1H NMR structure, and activity of a three-disulfide-bridged maurotoxin analog designed to restore the consensus motif of scorpion toxins. J. Biol. Chem. **275**, 13605–13612

4 Renisio, J., Romi-Lebrun, R., Blanc, E., Bornet, O., Nakajima, T. and Darbon, H. (2000) Solution structure of BmKTX, a K^+ blocker toxin from the Chinese scorpion *Buthus martensi*. Proteins **38**, 70–78

5 Pallaghy, P. K., Nielsen, K. J., Craik, D. J. and Norton, R. S. (1994) A common structural motif incorporating a cystine knot and a triple-stranded beta-sheet in toxic and inhibitory polypeptides. Protein Sci. **3**, 1833–1839

6 Norton, R. S. and Pallaghy, P. K. (1998) The cystine knot structure of ion channel toxins and related polypeptides. Toxicon **36**, 1573–1583

7 Craik, D. J., Daly, N. L. and Waine, C. (2001) The cystine knot motif in toxins and implications for drug design. Toxicon **39**, 43–60

8 Bernard, C., Legros, C., Ferrat, G., Bischoff, U., Marquardt, A., Pongs, O. and Darbon, H. (2000) Solution structure of hpTX2, a toxin from *Heteropoda venatoria* spider that blocks Kv4.2 potassium channel. Protein Sci. **9**, 2059–2067

9 Mosbah, A., Kharrat, R., Fajloun, Z., Renisio, J. G., Blanc, E., Sabatier, J. M., El Ayeb, M. and Darbon, H. (2000) A new fold in the scorpion toxin family, associated with an activity on a ryanodine-sensitive calcium channel. Proteins **40**, 436–442

10 Srinivasan, K. N., Sivaraja, V., Huys, I., Sasaki, T., Cheng, B., Kumar, T. K., Sato, K., Tytgat, J., Yu, C., Cheng San, B. et al. (2002) κ-Hefutoxin1, a novel toxin from the scorpion *Heterometrus fulvipes* with a unique structure and function: importance of the functional diad in potassium channel selectivity. J. Biol. Chem. **277**, 30040–30047

11 Liman, E. R., Tytgat, J. and Hess, P. (1992) Subunit stoichiometry of a mammalian K^+ channel determined by construction of multimeric cDNAs. Neuron **9**, 861–871

12 Marion, D., Ikura, M., Tschudin, R. and Bax, A. (1989) Rapid recording of 2D NMR spectra without phase cycling. Application to the study of hydrogen exchange in proteins. J. Magn. Res. **85**, 393–399

13 Marion, D. and Wüthrich, K. (1983) Application of phase sensitive two-dimensional correlated spectroscopy (COSY) for measurements of ^{1}H-^{1}H spin-spin coupling constants in proteins. Biochem. Biophys. Res. Commun. **113**, 967–974

14 Piotto, M., Saudek, V. and Sklenar, V. (1992) Gradient-tailored excitation for single-quantum NMR spectroscopy of aqueous solutions. J. Biomol. NMR **2**, 661–665

15 Bartels, C., Xia, T. H., Billeter, M., Guntert, P. and Wüthrich, K. (1995) The program XEASY for computer-supported NMR spectral analysis of biological macromolecules. J. Biomol. NMR **5**, 1–10

16 Wüthrich, K. (1986) NMR of Proteins and Nucleic Acids, Wiley, New York

17 Lecomte, C., Ferrat, G., Fajloun, Z., Van Rietschoten, J., Rochat, H., Martin-Eauclaire, M., Darbon, H. and Sabatier, J. M. (1999) Chemical synthesis and structure-activity relationships of Ts kappa, a novel scorpion toxin acting on apamin-sensitive SK channel. J. Pept. Res. **54**, 369–376

18 Bernard, C., Corzo, G., Mosbah, A., Nakajima, T. and Darbon, H. (2001) Solution structure of Ptu1, a toxin from the assassin bug *Peirates turpis* that blocks the voltage-sensitive calcium channel N-type. Biochemistry **40**, 12795–12800

19 Ferrat, G., Bernard, C., Fremont, V., Mullmann, T., Giangiacomo, K. and Darbon, H. (2001) Structural basis for alpha-K toxin specificity for K^+ channels revealed through the solution 1H NMR structures of two noxiustoxin-iberiotoxin chimeras. Biochemistry **40**, 10998–11006

20 Brunger, A. T., Adams, P. D., Clore, G. M., DeLano, W. L., Gros, P., Grosse-Kunstleve, R. W., Jiang, J. S., Kuszewski, J., Nilges, M., Pannu, N. S. et al. (1998) Crystallography & NMR system: a new software suite for macromolecular structure determination. Acta Crystallogr. D Biol. Crystallogr. **54**, 905–921

21 Roussel, A. and Cambillau, C. (1989) Silicon Graphics Geometry Partner Directory, pp. 77–78, Silicon Graphics, Mountain View, CA

22 Koradi, R., Billeter, M. and Wüthrich, K. (1996) MOLMOL: a program for display and analysis of macromolecular structures. J. Mol. Graphics **14**, 29–32

23 Laskowski, R., Rullmannn, J., MacArthur, M., Kaptein, R. and Thornton, J. (1996) AQUA and PROCHECK-NMR: programs for checking the quality of protein structures solved by NMR. J. Biomol. NMR **8**, 477–486

24 Kraulis, P. J. (1991) MOLSCRIPT: a program to produce both detailed and schematic plots of protein structures. J. Appl. Crystallogr. **24**, 946–950

25 Merritt, E. A. and Bacon, D. J. (1997) Raster3D: photorealistic molecular graphics. Methods Enzymol. **277**, 505–524

26 Nicholls, A., Sharp, K. A. and Honig, B. (1991) Protein folding and association: insights from the interfacial and thermodynamic properties of hydrocarbons. Proteins **11**, 281–296

27 Nicholls, A. and Honig, B. (1991) A rapid finite difference algorithm, utililizing successive over-relaxation to solve the Poisson-Boltzman equation. J. Comput. Chem. **12**, 435–445

28 Bernard, C., Corzo, G., Adachi-Akahane, S., Foures, G., Kanemaru, K., Furukawa, Y., Nakajima, T. and Darbon, H. (2004) Solution structure of ADO1, a toxin extracted from the saliva of the assassin bug, *Agriosphodrus dohrni*. Proteins **54**, 195–205

29 Guntert, P. and Wüthrich, K. (1991) Improved efficiency of protein structure calculations from NMR data using the program DIANA with redundant dihedral angle constraints. J. Biomol. NMR **1**, 447–456

30 Zhu, S., Darbon, H., Dyason, K., Verdonck, F. and Tytgat, J. (2003) Evolutionary origin of inhibitor cystine knot peptides. FASEB J. **17**, 1765–1767

31 Blanc, E., Sabatier, J. M., Kharrat, R., Meunier, S., El Ayeb, M., Van Rietschoten, J. and Darbon, H. (1997) Solution structure of maurotoxin, a scorpion toxin from *Scorpio maurus*, with high affinity for voltage-gated potassium channels. Proteins **29**, 321–333

32 Mouhat, S., Mosbah, A., Visan, V., Wulff, H., Delepierre, M., Darbon, H., Grissmer, S., De Waard, M. and Sabatier, J. M. (2004) The 'functional' dyad of scorpion toxin Pi1 is not itself a prerequisite for toxin binding to the voltage-gated Kv1.2 potassium channels. Biochem. J. **377**, 25–36

Received 7 October 2004/22 November 2004; accepted 5 January 2005
Published as BJ Immediate Publication 5 January 2005, DOI 10.1042/BJ20041705

© 2005 Biochemical Society